Loss of Rap1 Induces Telomere Recombination in the Absence of NHEJ or a DNA Damage Signal

Agnel Sfeir, *et al.*

Science **327**, 1657 (2010);
DOI: 10.1126/science.1185100

kinase contribute to the confinement of β_2AR-cAMP signaling.

One possible mechanism that might be responsible for T-tubule–selective β_2AR localization is the interaction of this receptor with lipid rafts (*11*). To investigate the role of these structures in the β_2AR localization and signaling, we performed SICM-FRET experiments in rat cardiomyocytes after membrane cholesterol depletion by methyl-β-cyclodextrin (MβCD). MβCD treatment did not cause any loss of T-tubules but induced β_2AR redistribution and propagation of β_2AR-cAMP signals from the crest of the cell (fig. S8), which suggested that the interaction of β_2ARs with cholesterol-rich membrane domains is important for normal β_2AR localization and signal compartmentation.

On the basis of the observed distribution of β_1 and β_2AR signals in failing versus healthy cardiomyocytes, we propose a model in which the compartmentation of the β_2AR-cAMP signaling changes in heart failure (fig. S9). Redistribution of the β_2AR from the T-tubules to the cell crest in failing cardiomyocytes and the loss of proper PKA localization, observed also in human heart failure (*24*), results in uncoupling of the β_2ARs from the localized pools of PKA that are responsible for the compartmentation of the β_2AR-cAMP signaling. Thus, in failing cells, activation of β_2ARs leads to cell-wide cAMP signal propagation patterns, similar to the patterns observed for β_1ARs (compare Fig. 4B and fig. S7D). Upon redistribution of the receptor, β_2AR signaling may lose its normally cardioprotective properties and may acquire the characteristics of the β_1AR response, thus contributing to the heart failure phenotype. It has been previously noted that β_2AR signals in ventricular myocytes from failing human hearts and animal heart failure models had functional effects more characteristic of the β_1AR (*25*, *26*). The propagating β_2AR-cAMP gradients that we observed in failing cardiomyocytes and in normal cardiomyocytes treated with rolipram or MβCD are compatible with the ability of β_2ARs to induce phospholamban and troponin I phosphorylation that was reported in these experimental settings and that is associated with arrhythmogenic effects of the β_2AR in heart failure (*27*–*30*).

In summary, using the SICM-FRET technique, we were able to functionally localize β_1ARs and β_2ARs to the surface structures of adult ventricular cardiomyocytes and to uncover the mechanisms leading to the abnormal cAMP compartmentation in heart failure. These findings should provide a deeper understanding of this cardiac disease and facilitate the development of new therapeutic strategies.

References and Notes

1. Y. Xiang, B. K. Kobilka, *Science* **300**, 1530 (2003).
2. R. P. Xiao, *Sci. STKE* **2001**, re15 (2001).
3. S. Engelhardt, L. Hein, F. Wiesmann, M. J. Lohse, *Proc. Natl. Acad. Sci. U.S.A.* **96**, 7059 (1999).
4. C. A. Milano *et al.*, *Science* **264**, 582 (1994).
5. C. Communal, K. Singh, D. B. Sawyer, W. S. Colucci, *Circulation* **100**, 2210 (1999).
6. W. Z. Zhu *et al.*, *Proc. Natl. Acad. Sci. U.S.A.* **98**, 1607 (2001).
7. V. O. Nikolaev, M. Bünemann, E. Schmitteckert, M. J. Lohse, S. Engelhardt, *Circ. Res.* **99**, 1084 (2006).
8. R. Fischmeister *et al.*, *Circ. Res.* **99**, 816 (2006).
9. M. J. Lohse, S. Engelhardt, T. Eschenhagen, *Circ. Res.* **93**, 896 (2003).
10. M. Zaccolo, T. Pozzan, *Science* **295**, 1711 (2002).
11. B. P. Head *et al.*, *J. Biol. Chem.* **280**, 31036 (2005).
12. I. L. Buxton, L. L. Brunton, *J. Biol. Chem.* **258**, 10233 (1983).
13. Materials and methods are available as supporting material on *Science* Online.
14. P. K. Hansma, B. Drake, O. Marti, S. A. Gould, C. B. Prater, *Science* **243**, 641 (1989).
15. Y. E. Korchev, Y. A. Negulyaev, C. R. Edwards, I. Vodyanoy, M. J. Lab, *Nat. Cell Biol.* **2**, 616 (2000).
16. P. Novak *et al.*, *Nat. Methods* **6**, 279 (2009).
17. A. R. Lyon *et al.*, *Proc. Natl. Acad. Sci. U.S.A.* **106**, 6854 (2009).
18. V. O. Nikolaev, M. Bünemann, L. Hein, A. Hannawacker, M. J. Lohse, *J. Biol. Chem.* **279**, 37215 (2004).
19. R. P. Xiao, X. Ji, E. G. Lakatta, *Mol. Pharmacol.* **47**, 322 (1995).
20. Y. Daaka, L. M. Luttrell, R. J. Lefkowitz, *Nature* **390**, 88 (1997).
21. M. Mongillo *et al.*, *Circ. Res.* **98**, 226 (2006).
22. J. J. Saucerman *et al.*, *Proc. Natl. Acad. Sci. U.S.A.* **103**, 12923 (2006).
23. M. A. Fink *et al.*, *Circ. Res.* **88**, 291 (2001).
24. D. R. Zakhary, C. S. Moravec, M. Bond, *Circulation* **101**, 1459 (2000).
25. F. del Monte *et al.*, *Circulation* **88**, 854 (1993).
26. G. W. Dorn 2nd, N. M. Tepe, J. N. Lorenz, W. J. Koch, S. B. Liggett, *Proc. Natl. Acad. Sci. U.S.A.* **96**, 6400 (1999).
27. J. DeSantiago *et al.*, *Circ. Res.* **102**, 1389 (2008).
28. D. Soto, V. De Arcangelis, J. Zhang, Y. Xiang, *Circ. Res.* **104**, 770 (2009).
29. S. Calaghan, L. Kozera, E. White, *J. Mol. Cell. Cardiol.* **45**, 88 (2008).
30. A. Kaumann *et al.*, *Circulation* **99**, 65 (1999).

31. We thank P. O'Gara for cardiomyocyte isolation; C. Dees for receptor binding assays; and L. Jaffe, F. Klauschen, and S. Gambaryan for critical reading of the manuscript. This study was supported by the Wellcome Trust (WTN 084064 to J.G.), Action Medical Research Grant (to J.G.), a U.K. Biotechnology and Biological Sciences Research Council grant (to Y.E.K.), a U.K. Medical Research Council grant (to J.G. and Y.E.K.) and a grant from Leducq Foundation (to S.E.H. and M.J.L.). Y.E.K. is a shareholder of, and P.N. has a consultancy agreement with, Ionscope Ltd., a company that sells scanning ion conductance microscopes. The cAMP sensor Epac2-camps used in this study is covered by a patent belonging to the University of Würzburg. It is being provided at no cost, but with a material transfer agreement, to nonprofit research institutes and universities.

Supporting Online Material

www.sciencemag.org/cgi/content/full/science.1185988/DC1
Materials and Methods
Figs. S1 to S9
References

26 May 2009; accepted 10 February 2010
Published online 25 February 2010;
10.1126/science.1185988
Include this information when citing this paper.

Loss of Rap1 Induces Telomere Recombination in the Absence of NHEJ or a DNA Damage Signal

Agnel Sfeir,* Shaheen Kabir,* Megan van Overbeek,† Giulia B. Celli, Titia de Lange‡

Shelterin is an essential telomeric protein complex that prevents DNA damage signaling and DNA repair at mammalian chromosome ends. Here we report on the role of the TRF2-interacting factor Rap1, a conserved shelterin subunit of unknown function. We removed Rap1 from mouse telomeres either through gene deletion or by replacing TRF2 with a mutant that does not bind Rap1. Rap1 was dispensable for the essential functions of TRF2—repression of ATM kinase signaling and nonhomologous end joining (NHEJ)—and mice lacking telomeric Rap1 were viable and fertile. However, Rap1 was critical for the repression of homology-directed repair (HDR), which can alter telomere length. The data reveal that HDR at telomeres can take place in the absence of DNA damage foci and underscore the functional compartmentalization within shelterin.

The shelterin subunit TRF2 is involved in the repression of the telomeric DNA damage response (*1*). Deletion of TRF2 results in activation of the ataxia telangiectasia mutated (ATM) kinase and telomere fusions mediated by nonhomologous end joining (NHEJ). TRF2 also contributes to the repression of homology-directed repair (HDR), which can create undesirable telomeric sister chromatid exchanges (T-SCEs). HDR at telomeres occurs in Ku70/80-deficient cells upon deletion of either TRF2 or the two POT1 proteins (*2*, *3*). The repression of ATM signaling, NHEJ, and HDR by TRF2 could potentially involve Rap1, which depends on TRF2 for its stable expression and recruitment to telomeres (*4*, *5*). Telo-

The Rockefeller University, 1230 York Avenue, New York, NY 10065, USA.

*These authors contributed equally to this work.
†Present address: Department of Molecular Biology, Memorial Sloan Kettering Cancer Center, 1275 York Avenue, New York, NY 10065, USA.
‡To whom correspondence should be addressed. E-mail: delange@mail.rockefeller.edu

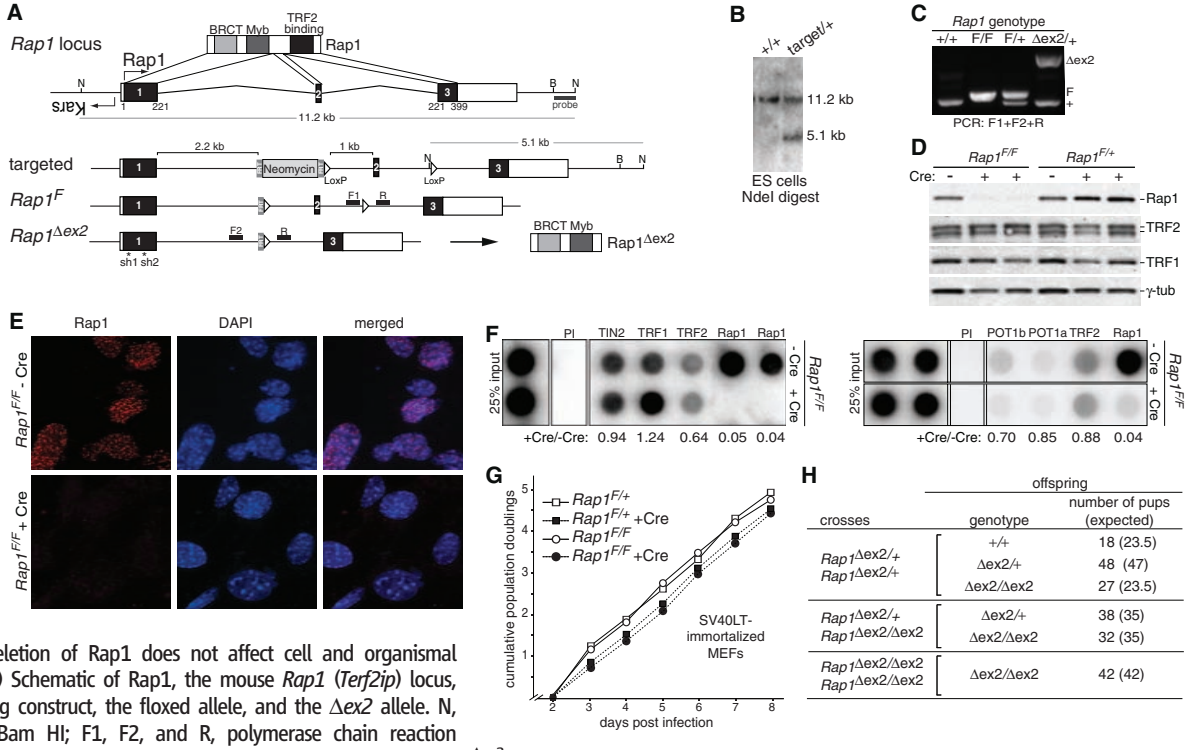

Fig. 1. Deletion of Rap1 does not affect cell and organismal viability. (**A**) Schematic of Rap1, the mouse *Rap1* (*Terf2ip*) locus, the targeting construct, the floxed allele, and the *Δex2* allele. N, Nde I; B, Bam HI; F1, F2, and R, polymerase chain reaction primers. Rap1 shRNAs are shown at the bottom. At right, $Rap1^{\Delta ex2}$-encoded protein. (**B**) Genomic blot of Nde I–digested DNA from embryonic stem (ES) cells. Probe is in (A). (**C**) Genotyping of tail DNAs. Primers are in (A). (**D**) Immunoblots for Rap1 (Ab1252), TRF2 (Ab1254), and TRF1 (Ab1449) from $Rap1^{F/F}$ and $Rap1^{F/+}$ MEFs 5 days after Hit-and-run (H&R)-Cre (first lane) or pWZL-Cre (second lane). (**E**) Loss of Rap1 IF signal from Cre-treated (day 5) $Rap1^{F/F}$ MEFs. Red, Rap1; green, telomeric fluorescence in situ hybridization (FISH); blue, DNA (DAPI, 4′,6′-diamidino-2-phenylindole). (**F**) Telomeric ChIPs on Cre-treated (day 5) $Rap1^{F/F}$ MEFs. Numbers represent ratios of percent telomeric DNA in the ChIPs [preimmune (PI) signal subtracted] on cells with (+) and without (–) Cre. (**G**) Proliferation of SV40LT-immortalized $Rap1^{F/F}$ and $Rap1^{F/+}$ MEFs infected as indicated. (**H**) Offspring from $Rap1^{\Delta ex2/+}$ and $Rap1^{\Delta ex2/\Delta ex2}$ intercrosses.

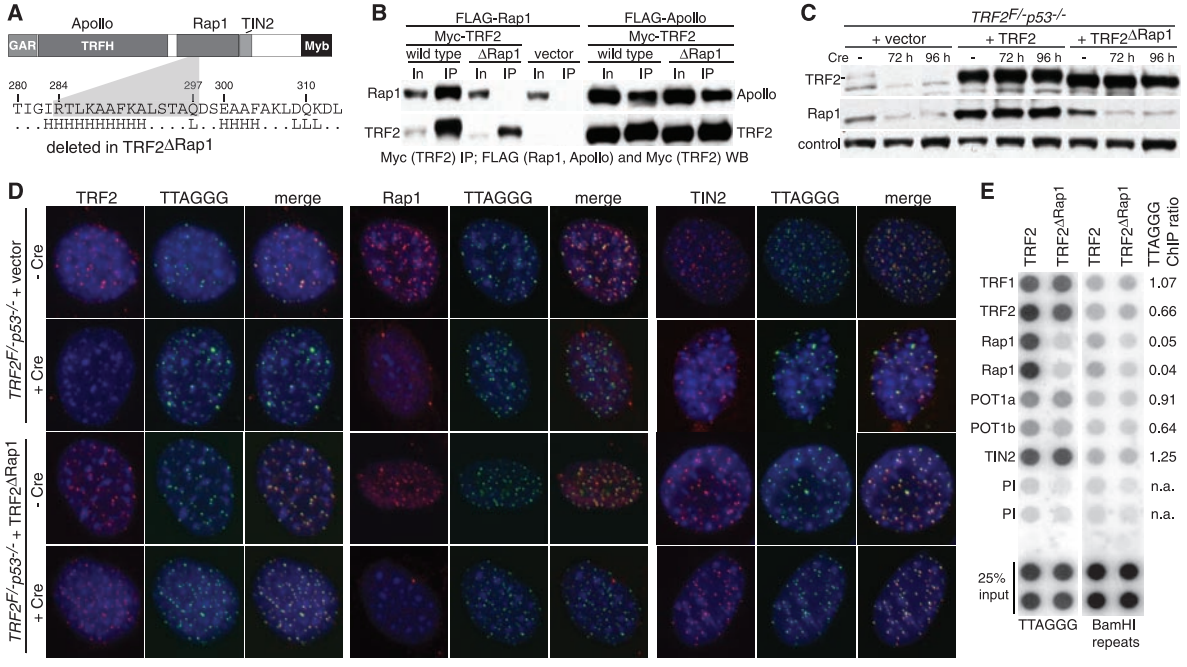

Fig. 2. A TRF2 mutant deficient for Rap1 binding. (**A**) The $TRF2^{\Delta Rap1}$ mutant. H, predicted helix. Amino acid residues: A, Ala; D, Asp; E, Glu; F, Phe; G, Gly; H, His; I, Ile; K, Lys; L, Leu; Q, Gln; R, Arg; S, Ser; and T, Thr. (**B**) Coimmunoprecipitation of Myc-TRF2 or Myc-$TRF2^{\Delta Rap1}$ with FLAG-Rap1 or FLAG-Apollo from cotransfected 293T cells. In, 2.5% of input. (**C**) Immunoblots for TRF2 and Rap1 from $TRF2^{F/-}p53^{-/-}$ MEFs expressing the indicated alleles at 72 and 96 hours after H&R-Cre. (**D**) IF-FISH to monitor TRF2, Rap1, and TIN2 at telomeres in $TRF2^{F/-}p53^{-/-}$ MEFs expressing $TRF2^{\Delta Rap1}$ or vector control at day 4 after Cre treatment. (**E**) Telomeric ChIP of $TRF2^{F/-}p53^{-/-}$ MEFs expressing TRF2 or $TRF2^{\Delta Rap1}$ at day 7 after Cre treatment. Duplicate dot blots were probed for telomeric DNA or the dispersed Bam HI repeats. ChIP ratios represent the percentage of telomeric DNA recovered in $TRF2^{\Delta Rap1}$- versus TRF2-expressing cells calculated as in Fig. 1.

mere protection is one of the functions of the distantly related Rap1 orthologs in yeast. In *Saccharomyces cerevisiae* and *Schizosccharomyces pombe*, Rap1 contributes to the repression of NHEJ at chromosome ends, whereas *Kluyveromyces lactis* Rap1 represses HDR (*6*–*9*). Human Rap1 affects telomere-length homeostasis and has been reported to repress telomere fusions (*10*–*12*). Here, we determined how Rap1 loss affects telomere function by generating mouse cells lacking a functional *Rap1* gene or lacking the endogenous TRF2 and complemented with a TRF2 mutant incapable of binding Rap1.

Because the first exon of the mouse *Rap1* gene immediately abuts the essential *Kars* lysyl–tRNA synthetase gene, we developed a conditional knockout strategy to delete exon 2 (Fig. 1, A to C). The $Rap1^{\Delta ex2}$ allele generated by Cre recombinase treatment of $Rap1^{F/F}$ cells can potentially encode a Rap1 fragment that lacks the TRF2-binding domain (Fig. 1A). We verified that this truncated form of Rap1, if it were produced, would not bind chromatin or localize to telomeres (fig. S1, A to C). Immunofluorescence (IF) and immunoblotting showed that Cre-treated SV40LT-immortalized $Rap1^{F/F}$ mouse embryonic fibroblasts (MEFs) indeed lacked any detectable Rap1 protein, and chromatin immunoprecipitation (ChIP) showed the loss of Rap1 from telomeres (Fig. 1, D to F, and fig. S1D). The expression and localization of other shelterin components were not significantly affected (Fig. 1, D to F, and fig. S1E).

The growth rate of the $Rap1^{\Delta ex2/\Delta ex2}$ MEFs was similar to that of control cells, regardless of whether the cells were immortalized with SV40LT, and primary MEFs lacking wild-type Rap1 did not show a growth arrest or p53 activation (Fig. 1G and fig. S1, F and G). Furthermore, $Rap1^{\Delta ex2/\Delta ex2}$ mice were born at the expected frequencies and were fertile (Fig. 1H). The survival of $Rap1^{\Delta ex2/\Delta ex2}$ cells and mice indicates that *Rap1* deletion does not result in major telomere dysfunction, which is known to be lethal. We further corroborated this conclusion by infecting $Rap1^{\Delta ex2/\Delta ex2}$ MEFs with a short hairpin RNA (shRNA)–targeting exon 1 (Fig. 1A and fig. S1H), which did not induce a growth arrest or other phenotypes typical of telomere dysfunction.

In the second approach to remove Rap1 from telomeres, we used previously characterized $TRF2^{F/-}p53^{-/-}$ MEFs (*4*) to replace the endogenous TRF2 with a mutant that does not bind to Rap1. A short predicted helix at position 290 in the previously mapped Rap1-binding

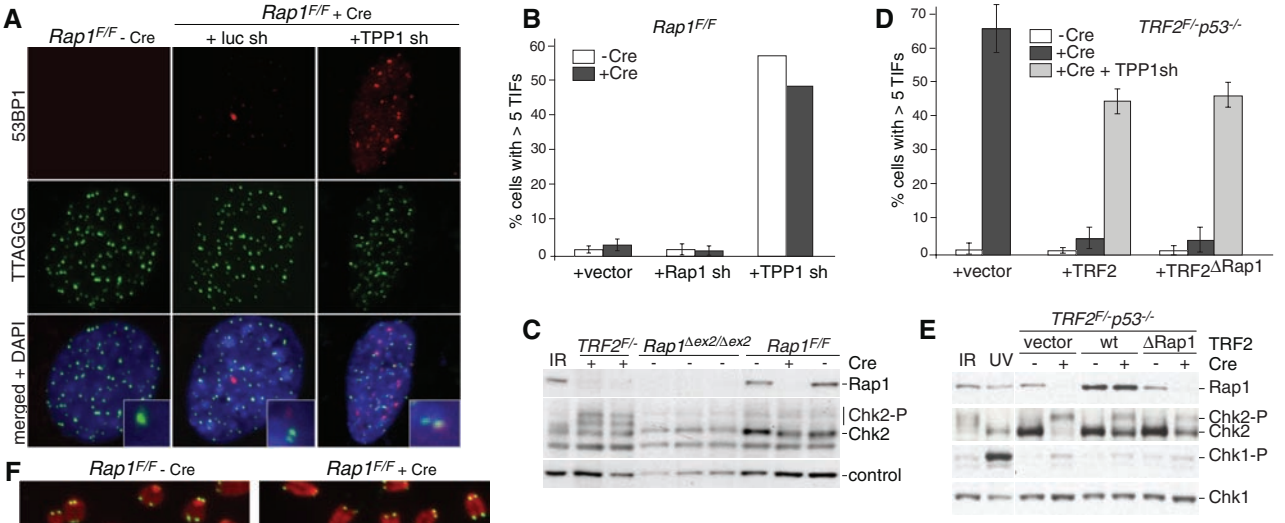

G *Rap1F/F*

Cre	shRNA	Telomeres scored	% fused (av)
-		800, 1030, 2124	0.13
+		2308, 4636, 5756	0.14
+	Rap1 sh	2720, 3452	0.19
-	TPP1 sh	1600, 2780	2.86
+	TPP1 sh	2240, 2860	2.93

H *TRF2F/-p53-/-*

TRF2 allele	Cre	shRNA	Telomeres scored	% fused (av±SD)
vector	-		3848, 3660, 2092	0.13 ± 0.05
	+		1808, 2176, 2004	49 ± 6.3
	+	TPP1 sh	1240, 1488, 1060	51 ± 2.2
TRF2	-		3628, 4312, 2124	0.03 ± 0.05
	+		4552, 2020, 2196	0.15 ± 0.19
	+	TPP1 sh	2520, 2880, 1780	1.65 ± 1.2
TRF2ΔRap1	-		3424, 4048, 2168	0.17 ± 0.07
	+		4428, 4140, 2212	0.06 ± 0.05
	+	TPP1 sh	2052, 2852, 1964	1.79 ± 0.2

Fig. 3. No DNA damage signal or NHEJ at the telomeres lacking Rap1. (**A**) TIF assay on $Rap1^{F/F}$ MEFs treated with Cre and the indicated shRNA. Red, IF for 53BP1; green, telomeric FISH; blue, DNA (DAPI). (**B**) TIF assay quantification. Mean ± SEM of two independent experiments ($n \geq 100$ nuclei each). (**C**) Chk2-P in Rap1-deficient MEFs. TRF2-null cells and ionizing radiation (IR)–treated cells [1 hour after 2-Gray (Gy) dose] serve as positive controls. (**D**) Quantification of TIF assays on $TRF2^{F/-}p53^{-/-}$ cells expressing TRF2, $TRF2^{\Delta Rap1}$, or vector control at day 4 after Cre treatement. Mean ± SD of three independent experiments ($n \geq 100$ nuclei each). (**E**) Chk1 and Chk2 phosphorylation in $TRF2^{F/-}p53^{-/-}$ MEFs expressing TRF2, $TRF2^{\Delta Rap1}$, or vector control. Ultraviolet (1 hour after 25 J/m^2 dose)– and IR (1 hour after 2-Gy dose)–treated cells serve as positive controls. (**F**) Metaphase chromosomes from $Rap1^{F/F}$ cells 5 days after Cre treatment. Red, DNA (DAPI); green, telomeric FISH. (**G**) Quantification of telomere fusions, detected as in (F) in $Rap1^{F/F}$ MEFs with the indicated Cre and shRNA treatments. Average (av) percentage of telomeres fused is given. (**H**) Quantification of telomere fusions in $TRF2^{F/-}p53^{-/-}$ MEFs [with (+) or without (–) Cre, day 4] complemented with TRF2 or $TRF2^{\Delta Rap1}$ or vector control and treated with TPP1 shRNA as indicated.

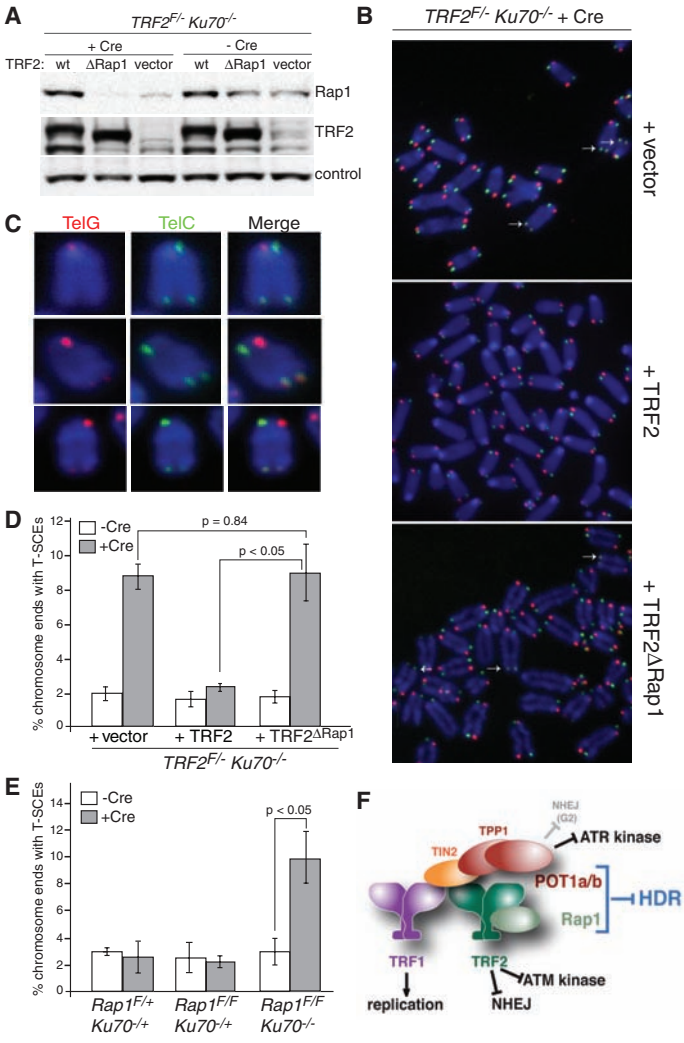

Fig. 4. Rap1 is a repressor of telomere recombination. (**A**) Rap1 and TRF2 from *TRF2*$^{F/-}$*Ku70*$^{-/-}$ MEFs expressing TRF2, TRF2$^{\Delta Rap1}$, or vector control analyzed 4 days after Cre treatment. (**B**) Chromosome orientation (CO) FISH analysis on cells as in (A). Arrows: T-SCEs. (**C**) Enlarged T-SCE events in Cre-treated TRF2$^{F/-}$Ku70$^{-/-}$ MEFs expressing TRF2$^{\Delta Rap1}$. (**D**) Quantification of T-SCEs as assessed in (B). Bars represent the mean ± SD from three independent experiments (n > 1100 chromosome ends each). P values are based on Student's two-tailed t test. (**E**) Quantification of T-SCEs as assessed in (B) in cells of the indicated Rap1 and Ku70 status. Method as in (D). Error bars: SEM (*Rap1*$^{F/+}$*Ku70*$^{-/+}$ and *Rap1*$^{F/F}$*Ku70*$^{-/+}$) or SD (*Rap1*$^{F/F}$*Ku70*$^{-/-}$). (**F**) The functions of shelterin components. See text for details.

region [amino acids 260 to 360 (*5*)] was conserved in TRF2 orthologs but not in TRF1 (fig. S2, A and B). Two mutations in this region (A289S and F290S) reduced the interaction between Rap1 and TRF2 in coimmunoprecipitation experiments (fig. S2C). To generate TRF2$^{\Delta Rap1}$, we deleted amino acids 284 to 297 (Fig. 2A). TRF2$^{\Delta Rap1}$ failed to bind to Rap1 in coimmunoprecipitation experiments, whereas it retained its interaction with Apollo (Fig. 2B). Wild-type TRF2 and TRF2$^{\Delta Rap1}$ were expressed in *TRF2*$^{F/-}$*p53*$^{-/-}$ MEFs, and the endogenous TRF2 was removed with Cre (Fig. 2C). Although TRF2$^{\Delta Rap1}$ localized to telomeres efficiently, IF and ChIP indicated that the telomeres lacked Rap1, and the overall abundance of Rap1 in the cells was reduced (Fig. 2, C to E, and fig. S3A). Other shelterin components were affected to an extent (less than twofold; Fig. 2, D and E) that is not expected to be functionally important because heterozygous MEFs and mice lacking one copy of *TRF1*, *TPP1*, *TRF2*, or *POT1a/b* display no telomere defect. Consistent with the viability of *Rap1*$^{\Delta ex2/\Delta ex2}$ cells, cells expressing TRF2$^{\Delta Rap1}$ proliferated at the same rate as cells expressing wild-type TRF2 (fig. S3B).

Rap1$^{\Delta ex2/\Delta ex2}$ cells did not show telomere dysfunction–induced foci [TIFs (*13*)], which are telomeric DNA damage foci that report on ATM and/or ATR (ataxia telangiectasia and Rad3-related) signaling at chromosome ends, and phosphorylation of Chk1 and Chk2 was not evident (Fig. 3, A to C). Further depletion of *Rap1* mRNA with an shRNA also failed to elicit a DNA damage signal in *Rap1*$^{\Delta ex2/\Delta ex2}$ cells (Fig. 3B). Consistent with these results, TRF2$^{\Delta Rap1}$ was equivalent to wild-type TRF2 in its ability to repress TIFs in cells lacking the endogenous TRF2 (Fig. 3D). The mutant form of TRF2 also repressed the induction of Chk-2 phosphorylation to the same extent as wild-type TRF2 (Fig. 3E). The low level of Chk2-P observed in Cre-treated TRF2- and TRF2$^{\Delta Rap1}$-expressing cells is likely due to Cre-induced DNA damage, because the phosphorylation of Chk2 was diminished when using a version of Cre that eventually disappears from the cells due to self-deletion (fig. S4). Furthermore, telomere fusions were not induced by deletion of *Rap1*, and TRF2$^{\Delta Rap1}$ had the same ability as wild-type TRF2 to repress NHEJ at telomeres (Fig. 3, F to H). However, because NHEJ of telomeres lacking TRF2 requires active DNA damage signaling (*14*), the lack of telomere fusions could be due to the lack of ATM or ATR activation. We therefore used a TPP1 shRNA to activate ATR kinase signaling at telomeres. This approach previously resulted in the reactivation of NHEJ at telomeres of cells lacking both TRF2 and ATM (*14*). Despite the telomeric ATR kinase signal elicited by the TPP1 shRNA (Fig. 3, B and D), Rap1 removal from telomeres did not induce their fusion (Fig. 3, G and H).

Thus, Rap1 does not appear to be required in the repression of either NHEJ or ATM kinase signaling, explaining why the deletion of Rap1 does not curb cellular or organismal viability. In addition, Rap1 was not required for the maintenance of several other features of mouse telomeres, including the maintenance of telomere length over three generations of mouse breeding and in cultured cells, the amount of single-stranded telomeric DNA, the telomeric nucleosomal organization, the methylation of telomeric H3K9, and the abundance of telomeric transcripts [TERRA (*15*)] (fig. S5).

HDR threatens telomere integrity because unequal T-SCEs can change telomere lengths. T-SCEs are most frequent when either *TRF2* or *POT1a/b* are deleted from Ku-deficient cells (*2*, *3*), although low frequency of T-SCEs have been reported for *POT1a* deficiency alone (*16*). To determine whether Rap1 was required for TRF2-mediated repression of T-SCEs, we introduced TRF2$^{\Delta Rap1}$ into SV40LT-immortalized *TRF2*$^{F/-}$*Ku70*$^{-/-}$ MEFs, which display frequent T-SCEs upon deletion of *TRF2* with Cre (*2*) (Fig. 4). Whereas the telomeric exchanges were repressed by wild-type TRF2, TRF2$^{\Delta Rap1}$ failed to block the telomeric HDR (Fig. 4, A to D). The frequency of T-SCEs was the same whether the cells expressed TRF2$^{\Delta Rap1}$ or no TRF2. Furthermore, T-SCEs were induced by Cre-mediated deletion of Rap1 from *Rap1*$^{F/F}$*Ku70*$^{-/-}$ cells (Fig. 4E). The T-SCEs occurred despite the absence of TIFs in cells lacking both Ku70 and telomeric Rap1 (fig. S6).

These data indicate that Rap1 functions at mouse telomeres to repress HDR, which has the potential for generating shortened telomeres and can promote telomerase-independent telomere maintenance. Rap1 appears to be an adaptor protein: Its C terminus serves to anchor the protein in shelterin; its BRCT domain, when dimerized in the shelterin complex, could bind a phosphorylated target protein; and the surface charge of its Myb-type motif makes it a third potential protein-interaction domain (*17*). As adaptors, the Rap1 orthologs could fulfill diverse functions in different organisms, because alterations in one of the protein-interaction domains could endow Rap1 with a new binding partner and thus instigate a new function.

These results underscore the functional compartmentalization within shelterin (Fig. 4F), which contains at least four subunits dedicated to distinct functions. The replication of telomeric

DNA is facilitated by TRF1 (*18*), and TPP1/POT1 are required for the repression of ATR signaling (*1*, *19*). TRF2 is the predominant repressor of both ATM signaling and NHEJ, and the current data show that these functions of TRF2 do not require Rap1. Finally, our results identify a fifth component of shelterin, Rap1, as an important repressor of HDR. Repression of HDR also requires TPP1/POT1 because removal of either Rap1 or POT1a/b result in telomere recombination. In a parallel pathway, Ku70/80 inhibits HDR, but it has not been established whether this function is telomere specific (*2*). This separation of function revealed that telomeres can undergo HDR without being detected by the ATM and ATR kinase pathways. When HDR takes place at telomeres lacking TRF2 or POT1a/b, DNA damage signaling results in the formation of TIFs. In the case of Rap1 removal, however, the telomeres lack detectable TIFs, yet are susceptible to HDR. Thus, consistent with the telomere recombination events in yeast lacking both Mec1 and Tel1 (*20*), the formation of DNA damage foci at telomeres is not a prerequisite for HDR.

References and Notes

1. T. de Lange, *Science* **326**, 948 (2009).
2. G. B. Celli, E. L. Denchi, T. de Lange, *Nat. Cell Biol.* **8**, 885 (2006).
3. W. Palm, D. Hockemeyer, T. Kibe, T. de Lange, *Mol. Cell. Biol.* **29**, 471 (2009).
4. G. B. Celli, T. de Lange, *Nat. Cell Biol.* **7**, 712 (2005).
5. B. Li, S. Oestreich, T. de Lange, *Cell* **101**, 471 (2000).
6. K. M. Miller, M. G. Ferreira, J. P. Cooper, *EMBO J.* **24**, 3128 (2005).
7. B. Pardo, S. Marcand, *EMBO J.* **24**, 3117 (2005).
8. S. Marcand, B. Pardo, A. Gratias, S. Cahun, I. Callebaut, *Genes Dev.* **22**, 1153 (2008).
9. A. J. Cesare, C. Groff-Vindman, S. A. Compton, M. J. McEachern, J. D. Griffith, *Mol. Cell. Biol.* **28**, 20 (2008).
10. B. Li, T. de Lange, *Mol. Biol. Cell* **14**, 5060 (2003).
11. M. S. O'Connor, A. Safari, H. Xin, D. Liu, Z. Songyang, *Proc. Natl. Acad. Sci. U.S.A.* **103**, 11874 (2006).
12. J. Sarthy, N. S. Bae, J. Scrafford, P. Baumann, *EMBO J.* **28**, 3390 (2009).
13. H. Takai, A. Smogorzewska, T. de Lange, *Curr. Biol.* **13**, 1549 (2003).
14. E. L. Denchi, T. de Lange, *Nature* **448**, 1068 (2007).
15. C. M. Azzalin, P. Reichenbach, L. Khoriauli, E. Giulotto, J. Lingner, *Science* **318**, 798 (2007).
16. L. Wu *et al.*, *Cell* **126**, 49 (2006).
17. S. Hanaoka *et al.*, *J. Mol. Biol.* **312**, 167 (2001).
18. A. Sfeir *et al.*, *Cell* **138**, 90 (2009).
19. T. Kibe, G. A. Osawa, C. E. Keegan, T. de Lange, *Mol. Cell. Biol.* **30**, 1059 (2010).
20. Y. L. Tsai, S. F. Tseng, S. H. Chang, C. C. Lin, S. C. Teng, *Mol. Cell. Biol.* **22**, 5679 (2002).

21. D. White, H. Takai, and the Rockefeller University Transgenics Facility are thanked for help in generating genetically modified mice. We thank L. Jovine for identifying the conserved helix in TRF2. A.S. is supported by Susan G. Komen for the Cure. G.B.C. was supported by the Women in Science Fellowship Program and The Leukemia & Lymphoma Society. Supported by NIH grants AG016642 and GM049046.

Supporting Online Material

www.sciencemag.org/cgi/content/full/327/5973/1657/DC1
Materials and Methods
Figs. S1 to S6
References

24 November 2009; accepted 24 February 2010
10.1126/science.1185100

Supporting Online Material for

Loss of Rap1 Induces Telomere Recombination in the Absence of NHEJ or a DNA Damage Signal

Agnel Sfeir, Shaheen Kabir, Megan van Overbeek, Giulia B. Celli, Titia de Lange*

*To whom correspondence should be addressed E-mail: delange@mail.rockefeller.edu

Published 26 March 2010, *Science* **327**, 1657 (2010)
DOI: 10.1126/science.1185100

This PDF file includes:

SFEIR ET AL. SUPPLEMENTARY MATERIALS

MATERIALS AND METHODS

Rap1 gene targeting

The *Rap1* targeting vector was generated by cloning restriction fragments from a BAC clone into the pSL301 vector (InVitrogen). A neomycin cassette flanked by 2 FRT sites and containing a LoxP site was inserted into a *Csp*CI site in the first intron. A second LoxP site, together with an *Nde*I site was introduced by inserting an oligonucleotide into a *BsmB*I site within the second intron. The vector was linearized with *Not*I and gene targeting of C57BL/6J ES cells was performed using standard techniques. ES cell clones with the correct integration were identified by southern blots of *Nde*I digested DNA using a 350-bp probe downstream of exon 3 outside the targeting vector. A correctly targeted ES clone was injected into C57BL/6J blastocyst to generate chimeric male founders. Crossing the chimeras to albino C57BL/6J females delivered offspring with the $Rap1^{F/+}$ genotype. Rap1 targeted mice were maintained in a C57BL/6J background. The neomycin cassette was deleted by crossing the mice to the FLPe-deleter mouse strain (Jackson Labs). The $Rap1^{\Delta ex2}$ allele was generated by crossing the $Rap1^{F/+}$ to the E2a-Cre deleter strain (Jackson Labs). $Rap1^{F/F}$ mice were crossed with $Ku70^{-/+}$ mice (obtained from F. Alt, Harvard Medical School, Boston MA) (*1)*. Genotyping PCR used the following primers: F1: 5'-CATGCACTTGTACACATACAA-3'; F2: 5'-GCTTCTTCCACCAAAACTGC-3'; and R: 5'-TTTGACAGTTGATAGGAAATGAAC-3'. PCR was performed in a volume of 25 μl containing 1 μl of DNA, 25 pmol of each primer, 0.1 μM dNTPs, 1.5 mM $MgCl_2$, 50 mM KCl, 10 mM Tris-HCl (pH 8.0), and 0.5 U of *Taq* polymerase (Takara Taq). Conditions were as follows: 95°C for 1 min, 35 rounds of 95°C for 30 s, 58°C for 45 sec, and 72°C for 45 sec and 72°C for 5 min.

Cell culture procedures and retroviral infection

MEFs were isolated from E13.5 embryos and maintained in DMEM supplemented with 1 mM Na-pyruvate, 100 U of penicillin per ml, 0.1 μg of streptomycin per ml, 0.2 mM L-glutamine, 0.1 mM nonessential amino acids, and 15% (vol/vol) fetal calf serum (FCS). Primary MEFs were immortalized by retroviral infection with pBabeSV40-LT (a gift from Greg Hannon) and cultured in media with 10% FCS without sodium pyruvate. $TRF2^{F/-}$ $p53^{-/-}$ and $TRF2^{F/-}Ku70^{-/-}$ MEFs were previously described (*2, 3)*. Cre recombinase was introduced using Hit&Run-Cre or pWZL-Cre as described previously (*2, 3)*. $TRF2^{\mathbf{F292S}}$ and $TRF2^{\mathbf{A289S}}$ were generated by site-directed mutagenesis. $TRF2^{\Delta Rap1}$ (lacking aa 284-297) was generated by ligating two PCR fragments, whereby nucleotides 851-891 were replaced by an *Nhe*I restriction site adding two residues (A,S) in place of amino acids 284-297. The different TRF2 mutations were cloned into pLPC-Myc retroviral expression vector. Full-length mouse Rap1 (aa 2-393) and Rap1-ex1 (aa 2-220) were cloned into pLPC-FLAG retroviral expression vector. Expression vectors were introduced into MEFs by 3 retroviral infections at 12-hr intervals using supernatant from transfected Phoenix cells. shRNA for TPP1 (GGACACATGGGCTGACGGA) (*4)* was introduced using 3 infections at 12-hr intervals of the shRNA bearing pSuperior-hygromycin retrovirus-containing supernatants from Phoenix cells. shRNA for *Rap1* (pLK0.1 from Open Biosystems; Sh1: ACAGGCAATGCCTTGTGGAAA; sh2: CTTCATCTCCA CGCAGTACAT) were introduced using 2 infections at 12-hr interval of lentivirus-containing supernatant generated in 293T cells. Viral supernatants were supplemented with 4 μg/ml polybrene. Infections were followed by puromycin selection for 3 days or hygromycin selection for 4 days.

Immunoblotting

Cells at the indicated time point and treatment were harvested by trypsinization, lysed in Laemmli buffer (100 mM Tris-HCl pH 6.8, 200 mM DTT, 3% SDS, 20% glycerol, 0.05% bromophenol blue) at $1*10^4$ cell per µl, denatured for 10 min at 95ºC, sheared with an insulin needle, and resolved on SDS/PAGE gels using the equivalent of $1*10^5$ cells per lane. After immunoblotting, the membranes were blocked in PBS with 5% non-fat dry milk/0.1%Tween and the following primary antibodies were incubated in PBS/5% non-fat dry milk/0.1% Tween: TRF1 (1449, rabbit polyclonal); TRF2 (1254, rabbit polyclonal); Rap1 (1252, rabbit polyclonal); POT1a (1221); POT1b (1223); Chk2 (mouse monoclonal, BD Biosciences); Phopho-Chk1 (Ser 345) (mouse monoclonal, Cell Signaling); Chk1 (mouse monoclonal, Santa Cruz); FLAG (M2, mouse monoclonal, Sigma); Myc (9E11 mouse monoclonal, Sigma); p53 (A1-25 mouse monoclonal; gift from K. Helin); γ-tubulin (clone GTU88, Sigma); α-tubulin (rabbit polyclonal; Sigma). After incubation with the appropriate secondary antibody, immunoblots were developed with enhanced chemiluminescence (ECL, Amersham).

Cell Fractionation

Cell fractionation experiments were performed as described by Mendez and Stillman (*5)*. Briefly, cells were collected by trypsinization, washed in PBS and incubated for 10 minutes in ice-cold buffer A (10 mM HEPES, pH 7.9, 10mM KCl, 1.5mM MgCl2, 0.34 M sucrose, 10% glycerol, 1 mM dithiothreitol, 1 mM phenylmethylsulfonyl fluoride, and a protease inhibitor mixture) containing 0.1 % Triton X-100. The cytoplasmic fraction was collected by centrifugation at 1300 *g* for 4 min. The cell pellet was then incubated with buffer B (3 mM, EDTA, 0.2 mM EGTA, 1 mM dithiothreitol, and the protease inhibitors described above) for 30 min. The lysate was fractionated to obtain nuclear fraction (supernatant) and chromatin bound fraction (pellet) by centrifugation at 1700 *g* for 4 min.

IF-FISH

IF-FISH to detect the telomeric localization of shelterin proteins and TIFs was performed as described previously (*6*). Cells grown on coverslips were fixed for 10 min in 2% paraformaldehyde at room temperature followed by three 5 min washes with PBS. Cells were incubated in blocking solution (1 mg/ml BSA, 3% goat serum, 0.1% Triton X-100, 1 mM EDTA in PBS) for 30 min, followed by incubation with primary antibodies in blocking solution for 1 hour at room temperature; 53BP1 (100-304) (Rabbit polyclonal, Novus Biological); γH2AX (JBW301) (Mouse monoclonal, Millipore). After washing with PBS three times, Cells were incubated with Rhoadamine Red-X labeled secondary antibody raised rabbit (RRX, Jackson) or Alexa Fluor 555 labeled secondary antibody raised mouse (Invitrogen) in blocking solution for 30 min at room temperature, and washed again with PBS three times. Coverslips were dehydrated with 70%, 95% and 100% ethanol, and allowed to dry up completely. Hybridizing solution (70% formamide, 0.5% blocking reagent (Roche), 10 mM Tris-HCl, pH 7.2, FITC-OO-(CCCTAAA)3 PNA probe (Applied Biosystems)) was added to each coverslips and heated for 10 min at 80^{o}C. After incubation for 2 hour at room temperature, cells were washed twice in washing solution (70% formamide, 10 mM Tris-HCl, pH 7.2), and three times in PBS. DNA was counterstained with DAPI and slides were mounted in anti-fade reagent (ProLong Gold, Invitrogen). Digital images were captured with a Zeiss Axioplan II microscope with a Hamamatsu C4742-95 camera using Improvision OpenLab software.

Telomeric ChIP analysis

Telomeric DNA CHIP was done as previously described (*7*). The following shelterin antibodies were used as crude sera: TRF1, 1449 (rabbit polyclonal); TRF2, 1254 (rabbit

polyclonal); Rap1, 1252 (rabbit polyclonal); POT1a, 1220 (rabbit polyclonal); POT1b, 1223 (rabbit polyclonal); TIN2, 1447 (rabbit polyclonal). Antibodies for H3 (1791), H3K9Me1 (9045), H3K9Me2 (1220) and H3K9Me3 (8898) were from Abcam.

Co-IPs from transfected 293T cells

2 x 10^6 293T cells were plated 24 h before co-transfection using calcium phosphate co-precipitation with 20 µg of pLPC-FLAG and pLPC-Myc constructs. Cells were harvested at 36 h after transfection, washed once with PBS, and lysed on ice for 10 min in a high salt buffer (50 mM Tris-HCl pH 7.2, 400 mM NaCl, 1% Triton X-100, 0.1% SDS, 1 mM EDTA, 1 mM DTT, 1 mM PMSF and cocktail of protease inhibitors). Salt concentration was brought down to 200 mM by addition of ice-cold water (drop-wise while mixing) and lysates were spun at 4°C at 14,000 rpm for 10 min. Supernatants were used in immunoprecipitations. 5 or 2.5% of the supernatant was saved as 'input' for western blot analysis and the remaining supernatant was pre-cleared with preblocked (10% BSA in PBS overnight) protein G-Sepharose beads for 1 h at 4°C. Lysates were incubated overnight at 4°C with a 40 µl slurry of Sepharose beads conjugated to 9E10-Myc or M2-FLAG mouse monoclonal antibody. Beads were washed 5 times with ice-cold PBS. Proteins were eluted by boiling for 5 min in 40 µl Laemmli buffer and analyzed by SDS-PAGE and immunoblotting.

FISH and CO-FISH

FISH and CO-FISH analysis of telomeric DNA was done as previously described (*2, 3)*. Briefly, colcemid was added for 2 hours prior to harvest. Cells were trypsinized, swollen in 0.075 M KCl, and fixed in methanol:acetic acid (3:1). Metaphase spreads were dropped on glass slides in a Thermotron Cycler (20^0C, 50% humidity) and aged overnight. The following day, the slides were hybridized with FITC-OO-$(CCCTAA)_3$ PNA

probe (Applied Biosystems) in hybridizing Solution (70% formamide, 1 mg/ml blocking reagent (Roche), 10 mM Tris-HCl pH 7.2) for 2 hours at rt. The slides were washed twice for 15 min in 70% formamide/10 mM Tris-HCl pH 7.2 followed by three 5 minutes washes in 0.1 M Tris-HCl, pH 7.0/0.15 M NaCl/0.08% Tween-20. 4,6-diamidino-2-phenylindole (DAPI) was added during the last wash to stain the chromosomes. Slides were mounted in antifade reagent (ProLong Gold, Invitrogen) and images were captured with a Zeiss Axioplan II microscope with a Hamamatsu C4742-95 camera. For CO-FISH, cells were incubated with 10 μM BrdU:BrdC (3:1) for 16 hrs prior to harvest. After processing the metaphase spreads to digest BrdU/dC substituted DNA strands with Exonuclease III, the slides were probed sequentially with TAMRAOO-$(TTAGGG)_3$ followed by FITC-OO-$(CCCTAA)_3$ PNA probe (2 hours each).

Analysis of telomere overhangs and telomere length

Analysis of telomeric overhang and telomere length was performed using pulse-field gel electrophoresis and in gel hybridization as previously described (*8)*.

MNase digestion

Telomeric nucleosomal configuration was assessed using MNase digestion assays following described protocols (*9)*.

Northern analysis for TERRA

Total cellular RNA was prepared using RNeasy Mini Kit (Qiagen), according to the manufacturer instructions and Northern blot analysis was performed as previously described (*10)*. Briefly, 10 μg RNA was loaded onto 1.3% formaldehyde agarose gels and separated by gel electrophoresis. RNA was transferred to a Hybond membrane.

The blot was prehybridized at 60°C for 1 h in Church mix (0.5 M Na_2HPO_4 (pH 7.2), 1 mM EDTA, 7% SDS, and 1% BSA), followed by hybridization at 60°C overnight with 800-bp telomeric DNA probe from pSP73Sty11 labeled using Klenow fragment, CCCTAA primers, and α-[^{32}P]-dCTP. The blot was exposed to a PhosphorImager screen and scanned using Image-Quant software.

SUPPLEMENTAL REFERENCES

1. Y. Gu *et al.*, *Immunity* **7**, 653 (1997).
2. G. Celli, T. de Lange, *Nat Cell Biol* **7**, 712 (2005).
3. G. B. Celli, E. Lazzerini Denchi, T. de Lange, *Nat Cell Biol* **8**, 885 (2006).
4. E. Lazzerini Denchi, T. de Lange, *Nature* **448**, 1068 (2007).
5. J. Mendez, B. Stillman, *Mol Cell Biol* **20**, 8602 (2000).
6. N. Dimitrova, T. de Lange, *Genes Dev* **20**, 3238 (2006).
7. D. Loayza, T. de Lange, *Nature* **424**, 1013 (2003).
8. D. Hockemeyer, J. P. Daniels, H. Takai, T. de Lange, *Cell* **126**, 63 (2006).
9. P. Wu, T. de Lange, *Mol Cell Biol* **28**, 5724 (2008).
10. C. M. Azzalin, P. Reichenbach, L. Khoriauli, E. Giulotto, J. Lingner, *Science* **318**, 798 (2007).

SUPPLEMENTAL FIGURE LEGENDS

fig. S1. Verification of the Rap1 knockout strategy.

(A) Immunoblot for Rap1 in cells expressing full length Rap1, Rap1-ex1, or vector control. The schematic below depicts full-length Rap1 protein (FLAG FL-Rap1) and the protein fragment encoded by exon 1 (FLAG Rap1-ex1). The antigenic region recognized by Rap1 Ab 1252 is indicated. (B) IF to monitor the localization of Rap1-ex1 and FL-Rap1. *Rap1*$^{\Delta ex2/\Delta ex2}$ MEFs expressing Rap1-ex1 or FL-Rap1 were assayed using FLAG (green) and TRF1 (red) antibodies. (C) *Rap1*$^{\Delta ex2/\Delta ex2}$ MEFs expressing FL-Rap1,Rap1-ex1, or vector control were fractionated as described in the materials and methods section and equal fractions of cytoplasmic proteins (CP), nucleoplasmic proteins (NP), and chromatin-bound proteins (CB) were analyzed by immunobloting with Rap1 Ab (1252) (D) Western blot showing the disappearance of full length Rap1 in cells deleted for exon 2. No new Rap1 protein was detected in cells bearing the *Rap1*$^{\Delta ex}$ allele. (E) Rap1$^{F/F}$ and Rap1$^{F/F}$ Ku$^{-/-}$ cells were fractionated on day 4 after Cre infection. The fractions were analyzed for the presence of POT1b and Rap1 by immunobloting. (F) FACS profiles of primary *Rap1*$^{F/F}$ cells infected with pWZL-Cre (lower panel) or vector control (upper panel) and analyzed at day 5 after infection. The percentage of G1, S and G2 cells is noted within the FACS profile. (G) Immunoblot for Rap1 and p53 on primary MEFs with the indicated genotype and Cre treatment (H) Western blot showing the effect of Rap1 shRNAs 1 and 2 on Rap1 levels in wild type MEFs. The mixture of the two shRNAs (mix) was used for the knockdown experiments in Fig. 3.

fig. S2. Identification of TRF2 residues required for Rap1 binding. (A) Schematic of TRF2 showing conservation of a subset of amino acids within the previously mapped Rap1 interaction domain. (B) Identification of a helical region within the conserved

segment. Predicted protein structure from PredictProtein.org. Mutations in the positions indicated in red affect Rap1 binding (see (C)). (C) Co-IPs of FLAG-tagged Rap1 with wild type TRF2, TRF2 mutants, or no protein from co-transfected 293T cells.

fig. S3. Cell proliferation not affected by TRF2$^{\Delta Rap1}$. (A) Immunoblots showing the expression of Rap1, TRF2, and TRF2$^{\Delta Rap1}$ in TRF2$^{F/-}$p53$^{-/-}$ MEFs treated with pWZL-Cre or the empty pWZL vector for the indicated time-periods. (B) Growth curve of cells shown in (A) and the vector controls.

fig. S4. TRF2$^{\Delta Rap1}$ does not induce Chk2 phosphorylation.

Rap1 and Chk2 immunoblots on TRF2$^{F/-}$p53$^{-/-}$ MEFs expressing TRF2, TRF2$^{\Delta Rap1}$, or vector control at 144 hours after treatment with Hit&Run-Cre.

fig. S5. No effect of Rap1 loss on telomere length, structure, and transcription.

(A) Telomeric restriction fragment analysis on cells isolated from liver of a *Rap1*$^{\Delta ex2/+}$ mouse and three successive generations of *Rap1*$^{\Delta ex2/\Delta ex2}$ mice. Telomeric DNA was detected by in-gel hybridization assays using a $(CCCAAT)_4$ probe under denaturing conditions. (B) Telomere length analysis on *Rap1*$^{\Delta ex2/\Delta ex2}$ MEFs and wild type cells at the indicated population doublings. (C) Telomere length analysis of *TRF2*$^{F/-}$ *p53*$^{-/-}$ cells expressing TRF2, TRF2$^{\Delta Rap1}$, or vector, plus or minus treatment with Cre. (D) Loss of Rap1 does not alter the telomeric single-stranded DNA signal. MEFs with the indicated genotypes were analyzed at day 5 post Cre treatment using in-gel hybridization to MboI digested DNA. The panel on the left shows the hybridization signal using a $(CCCAAT)_4$ probe under native conditions. The panel on the right represents total telomere signal after in situ denaturation of DNA and re-hybridization with the same probe. The numbers

on the bottom represent the relative overhang signal normalized to the total telomeric repeat signal. Values of the normalized signal are compared between – Cre (set at 1) and +Cre samples. (E) Unaltered nucleosomal organization of telomeric chromatin upon loss Rap1. DNA from MNase digested nuclei of $Rap1^{F/F}$ MEFs (+ or – Cre treatment) fractionated on a 1% agarose gel and stained with ethidium bromide (upper panel) to monitor organization of bulk nucleosomes or blotted and hybridized with a ^{32}P-$(CCCTAA)_4$ probe (lower panel). The two DNA samples marked by (*) were switched. The concentration of MNase ranged from 5 – 600 U/ml. (F) Rap1 loss has no effect on the heterochromatic marks at telomeres. Telomeric ChIP analysis of $Rap1^{F/F}$ cells treated with pWZL-Cre or H&R-Cre as indicated. Antibodies used are indicated on top. Pre-immune serum (PI) is used as a negative control. (G) Quantification of percentages of total telomeric DNA recovered in the ChIP shown in (F). (H) TERRA levels as detected by Northern blot analysis on Rap1 MEFs with the indicated genotype and Cre treatment. Ethidium bromide staining pattern serves as a loading control.

Fig. S6. No telomeric DNA damage signaling and normal telomere structure in cells deficient for Ku70 and telomeric Rap1.

(A) TIF assay on *$TRF2^{F/-}Ku70^{-/-}$* SV40LT-immortalized MEFs expressing TRF2, $TRF2^{\Delta Rap1}$, or vector control, 96 hr post Cre. Red, IF for 53BP1; green, telomeric FISH; blue, DNA (DAPI). (B) Quantification of TIF assay in (A). (C) Immunoblots for indicated shelterin components, Chk1, and Chk2 of the cells in (A). IR (1 hr post 2 Gy) and UV (1 hr post 25 J/m2) treated cells serve as positive controls. (D) Immunoblots for Rap1 and Chk2 on SV40LT-immortalized MEFs with the indicated genotypes, before and after treatment with Cre. (E) Loss of telomeric Rap1 in Ku70-deficient SV40LT-immortalized MEFs does not alter the telomeric single-stranded DNA signal. MEFs expressing TRF2, $TRF2^{\Delta Rap1}$, or vector control were analyzed using in-gel hybridization to MboI-digested

DNA before and 96 hours after treatment with Cre. Left, hybridization signal with $(CCCAAT)_4$ probe under native conditions; right, hybridization signal with same probe after in situ denaturation. Overhang signal was normalized to the total telomeric repeat signal. Numbers represent the relative overhang signal as compared to lane 4 (TRF2 plus Cre, set as 1).

SUPPLEMENTAL FIGURES S1-S6

fig. S1. Sfeir et al.

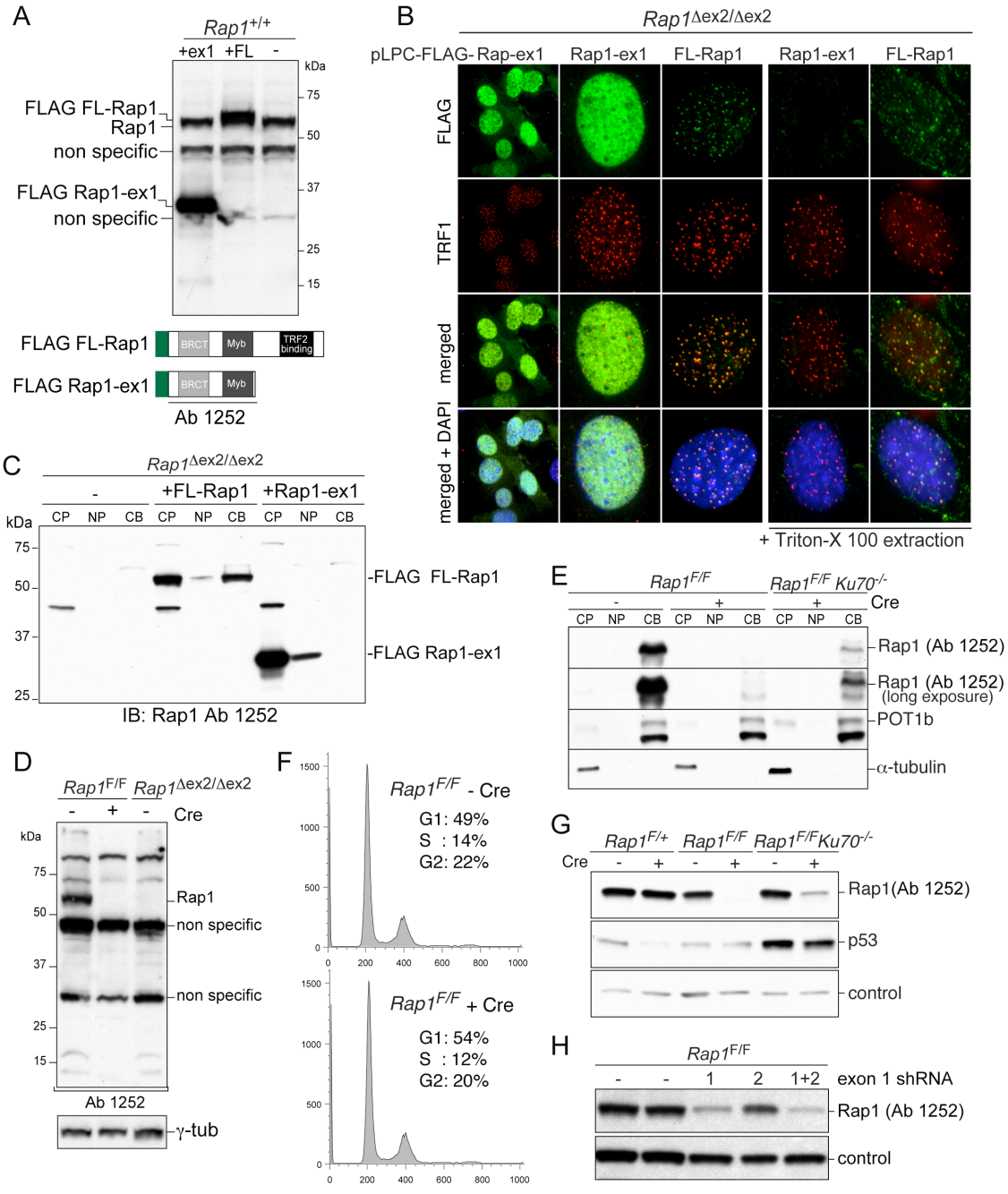

fig. S2. Sfeir et al.

A

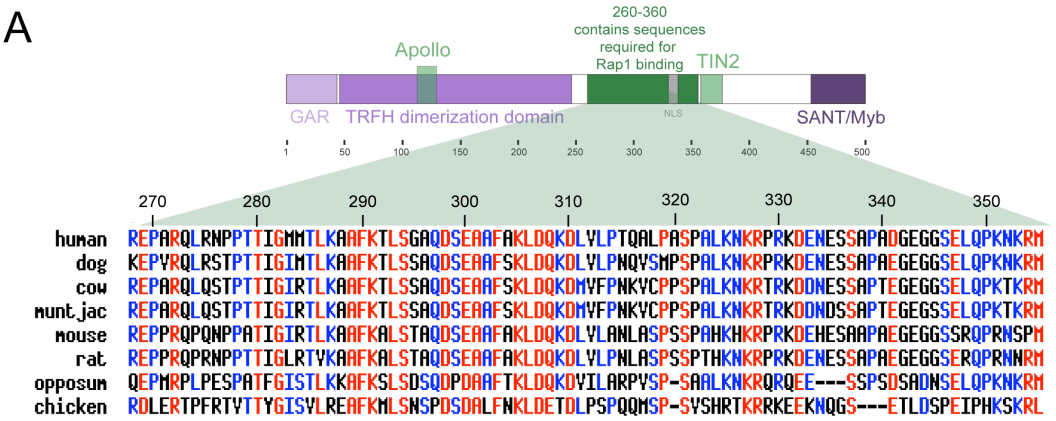

B

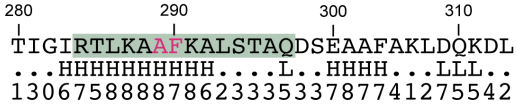

C

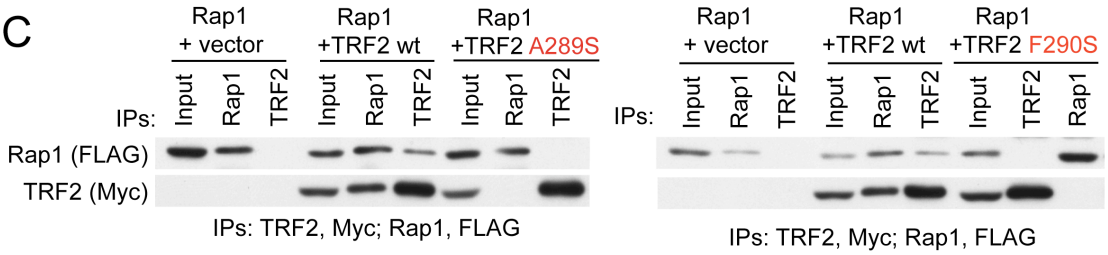

fig. S3. Sfeir et al.

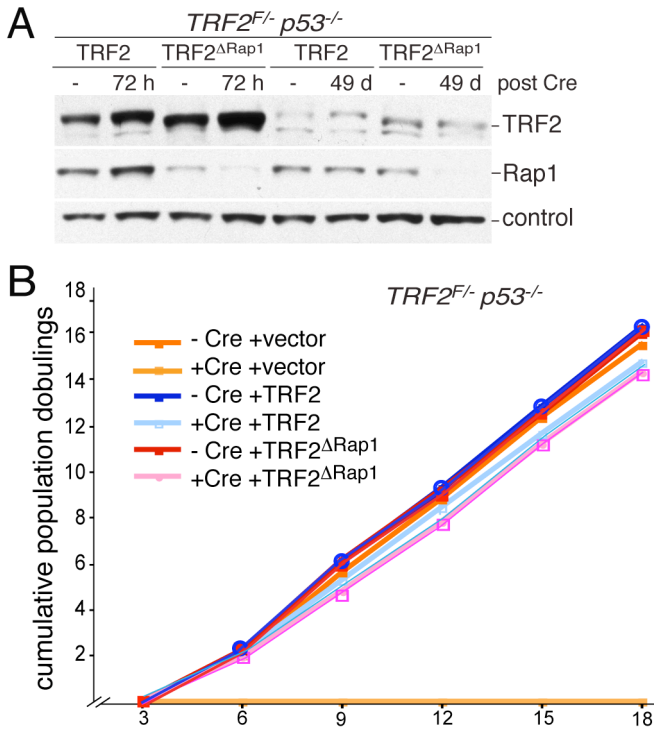

fig. S4. Sfeir et al.

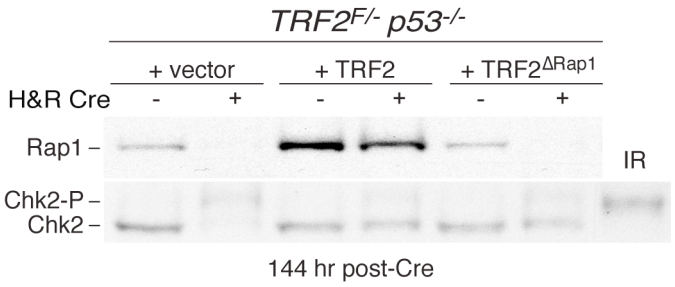

fig. S5. Sfeir et al.

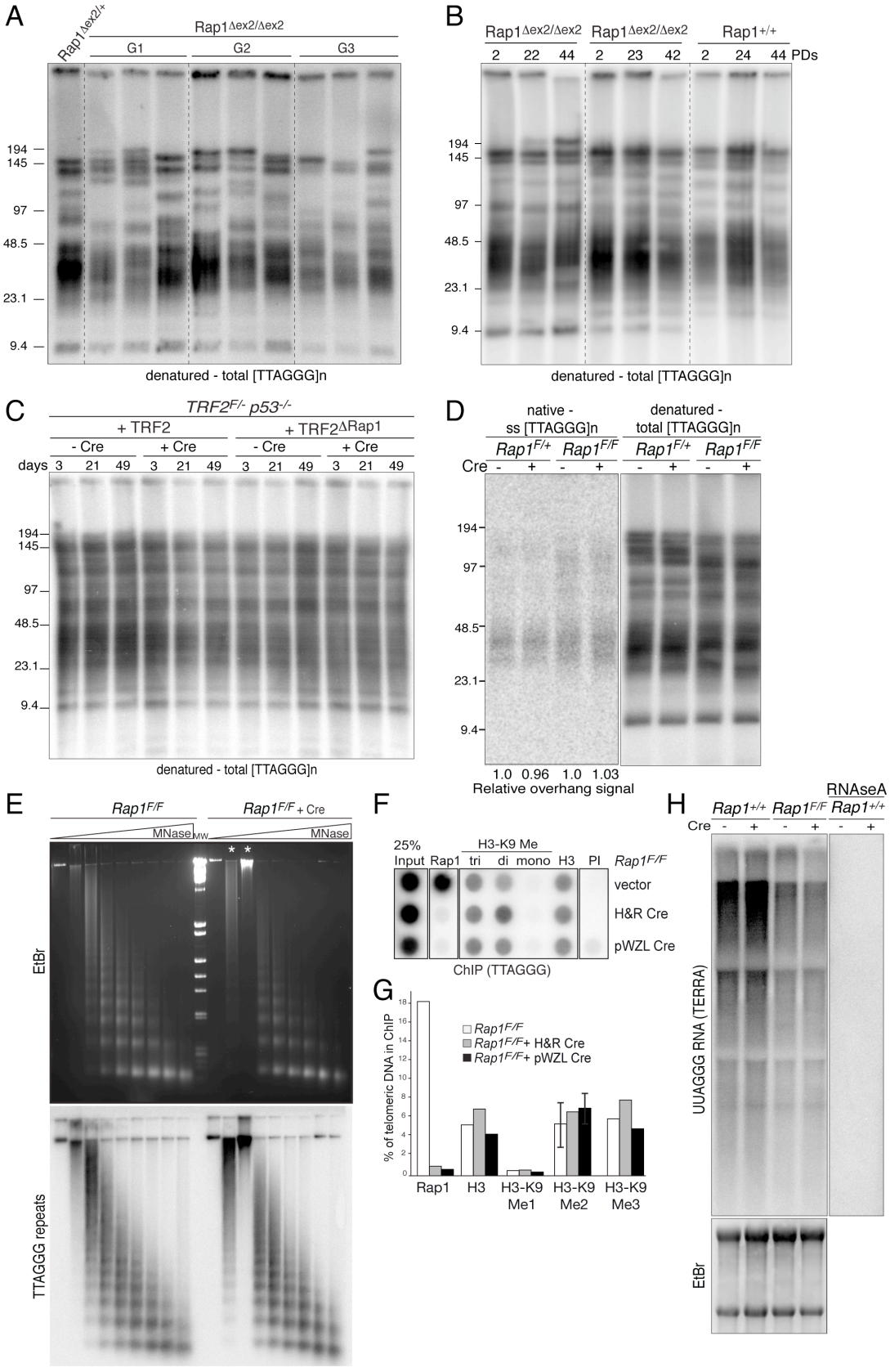

fig S6. Sfeir et al.